THE JOURNAL OF BIOLOGICAL CHEMISTRY VOL. 281, NO. 36, pp. 26280–26288, September 8, 2006
Printed in the U.S.A.

AtGRXcp, an *Arabidopsis* Chloroplastic Glutaredoxin, Is Critical for Protection against Protein Oxidative Damage*

Received for publication, February 13, 2006, and in revised form, June 16, 2006 Published, JBC Papers in Press, July 7, 2006, DOI 10.1074/jbc.M601354200

Ning-Hui Cheng[§1], **Jian-Zhong Liu**[‡], **Amanda Brock**[§], **Richard S. Nelson**[‡], **and Kendal D. Hirschi**[§¶‖]

From the [§]*Plant Physiology Group, United States Department of Agriculture/Agricultural Research Service Children's Nutrition Research Center, Department of Pediatrics, Baylor College of Medicine, Houston, Texas 77030,* [‡]*Plant Biology Division, Samuel Roberts Noble Foundation, Inc., Ardmore, Oklahoma 73401, the* [¶]*Department of Molecular and Human Genetics, Baylor College of Medicine, Houston, Texas 77030, and the* [‖]*Vegetable and Fruit Improvement Center, Texas A & M University, College Station, Texas 77845*

Glutaredoxins (Grxs) are ubiquitous small heat-stable disulfide oxidoreductases and members of the thioredoxin (Trx) fold protein family. In bacterial, yeast, and mammalian cells, Grxs appear to be involved in maintaining cellular redox homeostasis. However, in plants, the physiological roles of Grxs have not been fully characterized. Recently, an emerging subgroup of Grxs with one cysteine residue in the putative active motif (monothiol Grxs) has been identified but not well characterized. Here we demonstrate that a plant protein, AtGRXcp, is a chloroplast-localized monothiol Grx with high similarity to yeast Grx5. In yeast expression assays, AtGRXcp localized to the mitochondria and suppressed the sensitivity of yeast *grx5* cells to H_2O_2 and protein oxidation. AtGRXcp expression can also suppress iron accumulation and partially rescue the lysine auxotrophy of yeast *grx5* cells. Analysis of the conserved monothiol motif suggests that the cysteine residue affects *AtGRXcp* expression and stability. *In planta*, *AtGRXcp* expression was elevated in young cotyledons, green tissues, and vascular bundles. Analysis of *atgrxcp* plants demonstrated defects in early seedling growth under oxidative stresses. In addition, *atgrxcp* lines displayed increased protein carbonylation within chloroplasts. Thus, this work describes the initial functional characterization of a plant monothiol Grx and suggests a conserved biological function in protecting cells against protein oxidative damage.

Reactive oxygen species (ROS)[2] can be formed as by-products in all oxygenic organisms during aerobic metabolism (1). In higher plants, chloroplasts and mitochondria are two major organelles that contribute to production of reactive oxygen species during photosynthesis and carbon metabolism (2, 3). In addition, plants actively generate ROS as signals in response to environmental stresses (3–6). However, because of the cytotoxic and extremely reactive nature of ROS, they can cause wide ranging damage to macromolecules (1, 7–9). To overcome such oxidative damage and control signaling events, plants have orchestrated an elaborate antioxidant network (4).

Of those antioxidant systems, the physiological roles of thioredoxins have been intensively studied (10), whereas those of Grxs have not been fully defined (11, 12). Grxs are ubiquitous small heat-stable disulfide oxidoreductases, which are conserved in both prokaryotes and eukaryotes (11, 13). Through an active motif, namely the conserved CPYC sequence (a dithiol Grx), they catalyze the reduction of protein disulfides and of GSH-protein mixed disulfides via a dithiol or monothiol mechanism (14, 15). In bacterial, yeast, and mammalian cells, dithiol Grxs appear to be involved in many cellular processes and play an important role in protecting cells against oxidative stresses (16–18).

Besides the dithiol Grxs, a new group of monothiol Grxs has recently been identified in yeast (Grx3, -4, and -5) and bacteria (Grx4) that have a single cysteine residue in the putative active motif (19, 20). Yeast *Grx5* encodes a mitochondrial monothiol Grx, which is required for biogenesis of iron-sulfur clusters, whereas Grx3 and Grx4 function in detoxification of cytotoxin and cell proliferation in yeast (21–23). Interestingly, bacterial Grx4, unlike other previously characterized Grxs, can serve as a substrate for thioredoxin reductase instead of NADPH/glutathione reductase (20), suggesting that those monothiol Grxs have distinct functions. This group of monothiol Grxs is also conserved across organisms and has now been identified in malarial parasites, plants, zebrafish, mice, and humans (24–27). Recent studies also indicate that those Grxs contain a newly identified protein kinase C-interacting cousin of thioredoxin homology domain (PICOT-HD) in their carboxyl-terminal regions (24, 28). However, ascertaining a unifying function of PICOT-HD Grxs has been problematic.

Photosynthetic organisms, particularly higher plants, have a large Grx gene family; however, until recently, only a few plant Grxs have been studied (12, 29–30). In the *Arabidopsis* genome, there are at least 31 open reading frames coding for putative Grxs, which can be divided into three major classes that include the aforementioned monothiol Grxs (12, 30). Genetic analysis of a CC type *Grx*, *ROXY1*, indicates an important role of this protein in floral petal development (31). In a

* This work is supported by the United State Department of Agriculture/Agricultural Research Service under Cooperation Agreements 58-6250-6001K and 2004-34402-14768 and by National Science Foundation Grants 020977 and 0344350. The costs of publication of this article were defrayed in part by the payment of page charges. This article must therefore be hereby marked "*advertisement*" in accordance with 18 U.S.C. Section 1734 solely to indicate this fact.

[1] To whom correspondence should be addressed: Plant Physiology Group, USDA/ARS Children's Nutrition Research Center, Dept. of Pediatrics, Baylor College of Medicine, 1100 Bates St., Houston, TX 77030. Tel.: 713-798-7012; Fax: 713-798-7078; E-mail: ncheng@bcm.tmc.edu.

[2] The abbreviations used are: ROS, reactive oxygen species; PICOT-HD, protein kinase C-interacting cousin of thioredoxin homology domain; Grx, glutaredoxin; Trx, thioredoxin; GFP, green fluorescent protein; GUS, β-glucuronidase gene; CaMV, cauliflower mosaic virus promoter.

previous study, we used a yeast functional screen to identify a PICOT-HD-containing protein that was able to activate *Arabidopsis* CAX1 Ca^{2+}/H^{+} antiport activity in a yeast expression system; this gene was originally termed *CXIP1* (26). Here we determine the subcellular localization of this first cloned plant PICOT-HD-containing protein and reclassify the gene as *AtGRXcp*. We functionally characterize the protein and perform initial structure-function studies using yeast expression assays. We go on to isolate *AtGRXcp* knock-out mutants and describe the phenotypes of these plants at the whole plant and biochemical levels. For the first time, we demonstrate a role for a plant monothiol Grx.

EXPERIMENTAL PROCEDURES

Isolation of AtGRXcp Null Alleles—To isolate *atgrxcp* alleles, two T-DNA insertional mutant lines were obtained from the SALK T-DNA collection (32). Homozygous plants from each T_3 generation were obtained by PCR screening using *AtGRXcp*-specific and T-DNA border primers. An *AtGRXcp* reverse primer, 5′-GGG CCG GAT CCT CGA GTC AAG AGC ACA TAG CTT TCT C-3′, and a T-DNA left border primer, 5′-GCG TGG ACC GCT TGC TGC A-3′, were used to screen for the *atgrxcp1* allele. The *AtGRXcp* reverse primer and a T-DNA right border primer, 5′-TGG GAA AAC CTG GCG TTA CCC AAC TTA AT-3′, were used to screen for the *atgrxcp2* allele. An *AtGRXcp* forward primer, 5′-GGC AAG CTT ATA AGT TTT AAT CGT TTA TGG GGT-3′, and the *AtGRXcp* reverse primer were used to amplify the wild type *AtGRXcp* gene. The location of the T-DNA insertion was determined by sequencing the PCR product. Both *atgrxcp* alleles were back-crossed to their respective parental plants to remove any potential unlinked mutations.

Plant Growth Conditions—Arabidopsis wild type (ecotype Columbia, Col-0) and *atgrxcp* mutant seeds were surface-sterilized, germinated, and grown on one-half strength Murashige and Skoog medium (33) solidified with 0.8% agar and the same medium supplemented with various concentrations of H_2O_2. Iron-sufficient and -deficient media were made following a published protocol (34).

DNA Constructs and Site-directed Mutagenesis—Yeast *Grx5* was amplified by PCR using a forward primer (5′-GCC GGA TCC ATG TTT CTC CCA AAA TTC AAT-3′) and a reverse primer (5′-CCG GAG CTC TCA ACG ATC TTT GGT TTC TTC-3′), and the PCR products were cloned into pGEM-T Easy (Promega, Madison, WI). The full-length cDNA of *AtGRXcp* was isolated through a yeast functional screen and originally termed *CXIP1* (for CAX1-interacting protein 1) (26). AtGRXcp was predicted to have a 63-amino acid signal peptide by analysis with the Chloro P (version 1.1) program (available on the World Wide Web at www.cbs.dtu.dk/services/ChloroP/). To remove this N-terminal signal peptide, a truncated form of *AtGRXcp* was amplified by PCR using a forward primer (5′-GGG CTC GAG AGA TCT GCG ATG GCG TCG GCT CTT ACG CCG-3′) and the *AtGRXcp* reverse primer. Site-directed mutagenesis was performed as described previously (35). A forward primer (5′-GAA TCC CGT CTC CCC ATG GCT GGA TTC TCC AAC ACT GTG GTT CAG ATT TTG-3′) and a reverse primer (CGFS; 5′-GAA TTC CGT CTC CAT GGG GAA GTC TCT CGT TCC TTT C-3′) were used for creating the C97A mutation. A forward primer (5′-GAA TCC CGT CTC CCG ATG TGT GGA GCA TCC AAC ACT GTG GTT CAG ATT TTG-3′) and the reverse primer CGFS were used for creating the F99A mutation. The fidelity of all clones was confirmed by sequencing.

Yeast Strains, Expression Constructs, and Growth Assays—*Saccharomyces cerevisiae* wild type strain CML235 (*MAT*a *ura3–52 leu2Δ1 his3Δ200*), *grx5* (*MAT*a *ura3–52 leu2Δ1 his3Δ200 grx5*::*kanMX4*) were provided by Dr. Enrique Herrero (Universitat de Lleida, Lleida, Spain) and used in all yeast experiments. Yeast *Grx5* and *AtGRXcp* and its variants were cloned into piUGpd (36). Yeast cells were transformed by using the LiOAc method (37). All yeast strains were assayed on YPD medium (yeast peptone dextrose, rich medium), with or without various concentrations of H_2O_2, and SC medium plus six amino acids or five amino acids without lysine (21, 26).

Localization of AtGRXcp-Green Fluorescent Protein (GFP) Fusions in Yeast and Plant Cells—Full-length and truncated *AtGRXcp* and its variants were fused to the N terminus of green fluorescent protein (GFP) using a procedure described previously (38). The GFP constructs were subcloned into yeast and plant expression vectors as described previously (38). The subcellular localization of the fused proteins was imaged in comparison with labeled organelle markers (chloroplasts, mitochondria, Golgi, and peroxisome) as described previously (38). A peroxisome-targeted DsRed (red fluorescent protein), DsRed-per, was constructed by adding the plant peroxisome-targeting signal, KSRM, to the end of DsRed (39). The fluorescence signals were detected at 510 nm (excitation at 488 nm) for GFP, at 582 nm (excitation at 543 nm) for DsRed, and at 660 nm (excitation at 633 nm) for chlorophyll using Leica TCS SP2 AOBS confocal laser-scanning microscope. The fluorescence intensities were quantified by using the LCS software.

AtGRXcp::GUS Transgenic Plants—A 397-bp DNA sequence upstream of ATG of *AtGRXcp* open reading frames was amplified from genomic DNA by using the following primer sets: forward primer (5′-GGC AAG CTT ATA AGT TTT AAT CGT TTA TGG GGT-3′) and reverse primer (5′-GCC TCT AGA TTT TGA CGA CTT TTA GAT TTG GAA-3′). The PCR fragment was cloned into pBI121 to replace the 35S CaMV promoter, resulting in plasmid p*AtGRXcp*::GUS. Agrobacterium transformation of *Arabidopsis* plants was performed as described previously (40). More than 50 T2 generation plants were selected for Kan resistance.

Protein Oxidation Analysis—Carbonyl assays for analysis of oxidized proteins in both yeast and plant cells were performed as previously described (19, 41, 42). Yeast cultures of the strains (CML235 and *grx5*) expressing vector, *Grx5*, and *AtGRXcp* were grown in YPD media overnight at 30 °C. Half of the culture of each strain was subjected to treatment with 5 mM H_2O_2 for 1 h. Total proteins were extracted from cells with and without treatment. Western blot analysis was used to determine carbonyl group content. Arabidopsis chloroplasts were isolated from photosynthetic tissues of 6-week-old flowering wild type-, *atgrxcp*-, and *AtGRXcp*-overexpressing plants (43). The oxidized proteins were detected by protein gel blotting using anti-

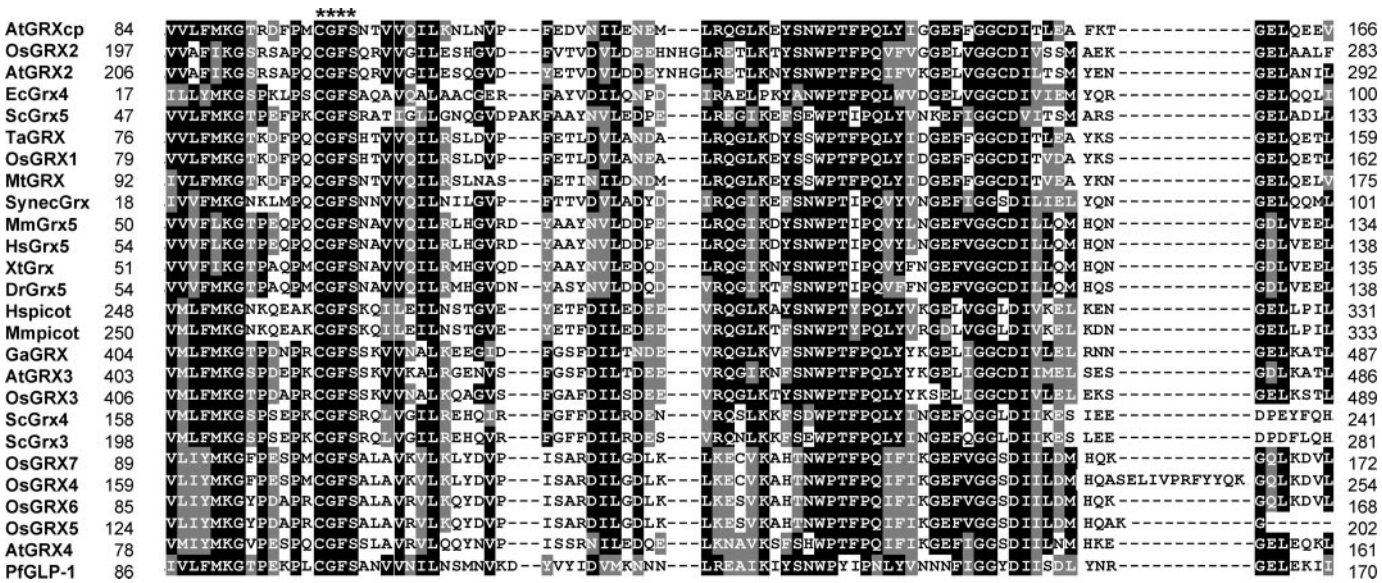

FIGURE 1. **Sequence analyses of monothiol Grxs.** Alignment of monothiol Grx sequences was performed with ClustalW software (available on the World Wide Web at www.ebi.ac.uk/clustalw/). The conserved putative monothiol active motif CGFS is indicated by *asterisks*. Accession numbers are as follows: AtGRXcp (AY157988), AtGRX2 (AY157989), AtGRX3 (ADD17344), AtGRX4 (BAB02297), EcGrx4 (P37010), DrGrx5 (AAZ30729), GaGRX (Tc29218), Hspicot (AAF28844), HsGrx5 (AAH47680), Mmpicot (AAF28842), MmGrx5 (Q80Y14), MtGRX (Tc102010), OsGRX1 (AAO20065), OsGRX2 (ABA96598), OsGRX3 (AAM93692), OsGRX4 (BAB62565), OsGRX5 (BAB91855), OsGRX6 (BAD87472), OsGRX7 (BAD68123), PfGLP-1 (CAB38997), ScGrx3 (Q03835), ScGrx4 (P32642), ScGrx5 (Q02784), SynecGrx (AAD19873), TaGRX (Tc254245), and XtGrx (AAH75374), where At represents *Arabidopsis thaliana*, Dr is *Danio rerio*, Ec is *Escherichia coli*, Ga is *Gossypium arboretum*, Hs is *Homo sapiens*, Mm is *Mus musculus*, Mt is *Medicago truncatula*, Os is *Oryza sativa*, Pf is *Plasmodium falciparum*, Sc is *Saccharomyces cerevisiae*, Synec is *Synechocystis*, Ta is *Triticum aestivum*, and Xt is *Xenopus tropicalis*.

dinitrophenylhydrazone antibody (42) (Bethyl Laboratory, Montgomery, TX).

Measurement of Iron Concentration—Yeast strains (CML235 and *grx5*) expressing vector, *Grx5*, and *AtGRXcp* were grown in 50 ml of selection media (−Ura) overnight at 30 °C. Each yeast culture was inoculated into 300 ml of YPD medium and grown until an A_{600} of 1.0 was reached. Yeast cells were harvested and washed and dried at 70 °C and subjected to inductively coupled plasma spectrometry analysis (44). To determine the soluble iron concentration, cells were sonicated and broken with a Sonic Dismembrator (Fisher), and the intracellular iron content was examined with a QuantiChron™ iron assay kit (BioAssay Systems, Hayward, CA).

RESULTS

AtGRXcp Is a Member of the Monothiol Glutaredoxins—CXIP1 (CAX-interacting protein 1; accession number AY157988) was originally identified based on its function in a yeast assay (26); however, we propose that CXIP1 should be reclassified as AtGRXcp. Our computational analysis revealed that AtGRXcp is similar to yeast monothiol Grxs (Grx3, -4, and -5), bacterial Grx4, PfGLP-1 from a malarial parasite, and both zebrafish and mice Grx5 (Fig. 1). This group of monothiol Grxs also contains a PICOT-HD, which is conserved in PICOTs from mammalian cells and plants (28). Several Grxs, like yeast Grx3 and -4, and human PICOT, have an N-terminal extension; however, AtGRXcp, similar to the bacterial Grx4, and both yeast and zebrafish Grx5, does not contain the N-terminal extension (Fig. 1) (19, 20, 27). In addition, our analysis suggests that in higher plants, these monothiol Grxs exist in both monocots and dicots (Fig. 1). In *Arabidopsis*, there are four members of these Grxs (Fig. 1). A dithiol Grx has two cysteine residues in the active motif that are able to catalyze protein disulfides and GSH-protein mixed disulfides (11, 17, 18); however, the subfamily of Grxs has only one conserved cysteine residue in the putative active motif, termed "CGFS" (Fig. 1). These observations indicate that monothiol Grxs are also conserved throughout prokaryotes and eukaryotes (Fig. 1). Based on the sequence analysis of those Grxs, we conclude that AtGRXcp is the first cloned plant monothiol Grx.

AtGRXcp Is a Chloroplast-localized Monothiol Grx—Monothiol Grxs have a diverse subcellular distribution in multiple organisms. For example, yeast Grx5 is mitochondria-localized (21), and Grx3 targets to nuclei (45), whereas a human PICOT is located in the cytosol (24). In order to gain insight into the function of AtGRXcp, we fused it with GFP at its C terminus and transiently expressed this fusion protein in tobacco leaf cells. Using various organelle markers, AtGRXcp-GFP was shown to clearly target to chloroplasts rather than mitochondria, Golgi, or peroxisomes in mesophyll cells (Fig. 2*A*). Analysis of the AtGRXcp sequence predicts that a 63-amino acid signal peptide is present at the N terminus (data not shown). To experimentally verify this, we removed this putative signal peptide and fused the truncated AtGRXcp (AtGRXcpΔ63) with GFP for transient expression in tobacco cells. As shown in Fig. 2*B*, AtGRXcpΔ63-GFP no longer targeted to chloroplasts and instead was dispersed throughout the cytosol and nuclei, similar to observations with free GFP (Fig. 2*B*, data not shown).

AtGRXcp Suppresses the Sensitivity of a Yeast grx5 Mutant to H_2O_2—Yeast *grx5* cells are growth-impaired in minimal medium and sensitive to oxidative stresses (19, 21). To examine if AtGRXcp could restore Grx5 function and suppress the sensitivity of *grx5* cells to an external oxidant, H_2O_2, we expressed

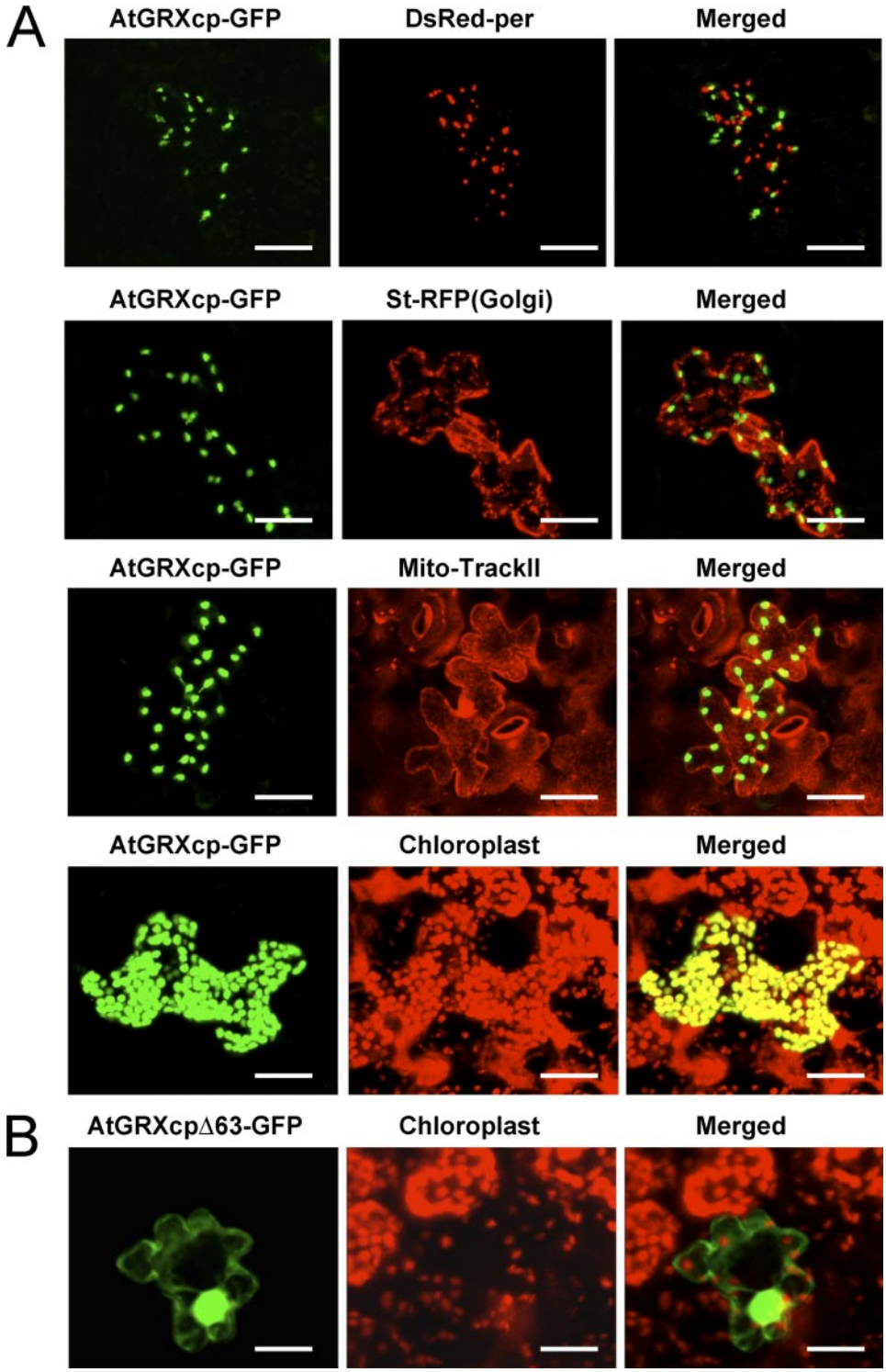

FIGURE 2. **Subcellular localization of AtGRXcp-GFP in plant cells.** *A*, AtGRXcp-GFP is localized to chloroplasts in tobacco cells. The *left panels* display the transient expression of AtGRXcp-GFP in tobacco cells; *central panels* display fluorescence from individually labeled markers for plant organelles or fluorescing chloroplasts; and *right panels* show the *merged images*. *B*, a truncated AtGRXcp-GFP fusion is not targeting to chloroplasts. *Scale bars*, 25 μm.

vector control, *AtGRXcp*, and yeast endogenous *Grx5* in *grx5* cells. All yeast strains grew normally in YPD liquid media (rich media) after 48 h of growth (Fig. 3*A*). Whereas vector-expressing *grx5* cells were growth-impaired in the medium with 3 mM H_2O_2, both *AtGRXcp*- and *Grx5*-expressing *grx5* cells grew in a similar manner to wild type cells (Fig. 3*A*). These observations suggest that AtGRXcp is able to suppress the sensitivity of *grx5* cells to oxidative stress.

Given that AtGRXcp localized to chloroplasts, which are specific to plants (Fig. 2) and yeast Grx5 is a mitochondrial Grx (21), the suppression of *grx5* phenotypes mandates that the subcellular localization of AtGRXcp in yeast cells differs from that seen in plants. To investigate this, AtGRXcp-GFP was expressed in yeast cells. Yeast growth assays revealed that AtGRXcp-GFP was functional and could suppress the sensitivity of *grx5* cells to H_2O_2 (Fig. 3*B*). Through immunolabeling studies, AtGRXcp-GFP localized to mitochondria in yeast cells, whereas a truncated AtGRXcpΔ63-GFP was unable to target to this organelle (Fig. 3*C*). Targeting of AtGRXcp to mitochondria was essential for the function of this protein in yeast, since both AtGRXcpΔ63 and AtGRXcpΔ63-GFP were unable to suppress the sensitivity of *grx5* cells to H_2O_2 (Fig. 3, *A* and *B*).

AtGRXcp Is Able to Protect Cells against Protein Oxidation and Rescue the Lysine Auxotrophy of a Yeast grx5 Mutant—In *grx5* cells, total protein carbonyl content is significantly increased under oxidative stress (Fig. 4*A*), suggesting that yeast Grx5 plays a vital role in directly protecting enzymes from oxidative damages (19, 21). In order to determine if AtGRXcp could directly reduce protein carbonylation in the *grx5* cells, we performed Western blot analysis of total proteins isolated from vector-, *AtGRXcp*- and *Grx5*-expressing *grx5* cells grown in H_2O_2-containing YPD media. Oxidized protein content in *AtGRXcp*-expressing cells was reduced compared with the vector-expressing cells but similar to *Grx5*-expressing cells (Fig. 4*A*). These results demonstrate that AtGRXcp can protect cells against protein oxidative damages.

Yeast Grx5 is a mitochondrial Grx required for the maturation of Fe-S clusters (21, 46). Deletion of *Grx5* results in inactivation of the mitochondrial Fe-S enzyme homoaconitase,

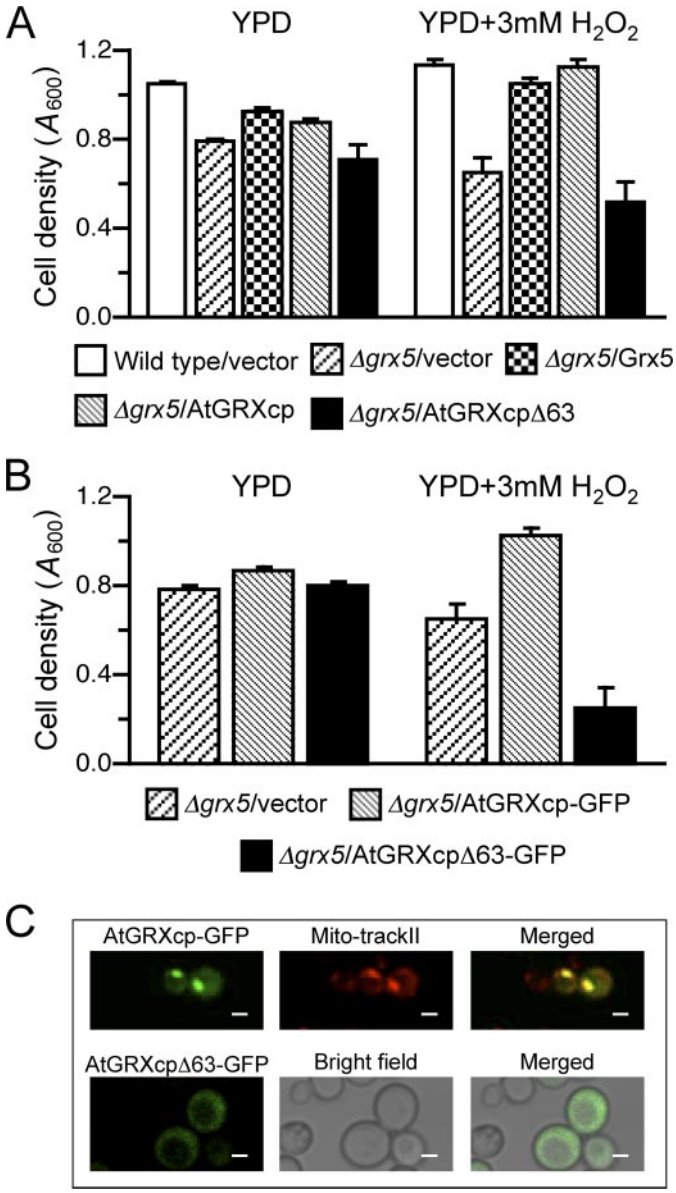

FIGURE 3. **AtGRXcp is able to suppress the sensitivity of *grx5* cells to H_2O_2.** *A* and *B*, vector-expressing wild type cells and vector-, *AtGRXcp-*, *AtGRXcp-GFP-*, *AtGRXcpΔ63-*, *AtGRXcpΔ63-GFP-*, and *Grx5*-expressing *grx5* cells were grown in YPD liquid media and the same media supplemented with 3.0 mM H_2O_2. Cell density was measured at A_{600} after 48 h of growth at 30 °C. Shown are two representative experiments from four independent experiments conducted. The *bars* indicate the S.E. ($n = 8$). *C*, subcellular localization of AtGRXcp-GFP (*top*) and AtGRXcpΔ63-GFP (*bottom*) in yeast cells. *Scale bars*, 10 μm.

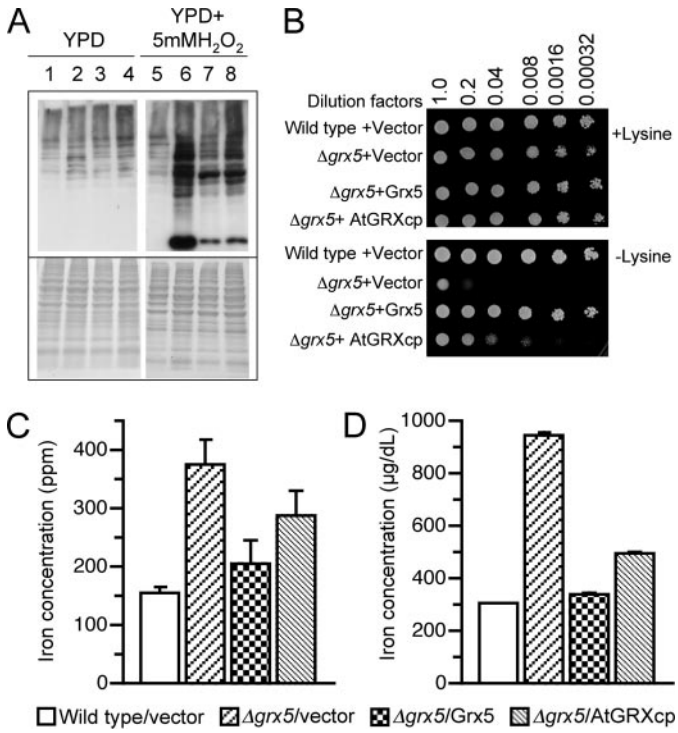

FIGURE 4. **AtGRXcp can suppress yeast *grx5* phenotypes.** *A*, protein carbonyl contents were analyzed by Western blotting with anti-dinitrophenylhydrazone antibody (1:1000). A parallel run stained with Coomassie Brilliant Blue is shown in the *bottom panel*. Total proteins were extracted from vector-expressing wild type strain (*lanes 1* and *5*) and vector-expressing (*lanes 2* and *6*), *Grx5*-expressing (*lanes 3* and *7*), and *AtGRXcp*-expressing (*lanes 4* and *8*) *grx5* cells. *B*, AtGRXcp partially rescues the lysine auxotrophy of the yeast *grx5* mutant. *grx5* cells expressing vector, *Grx5*, and *AtGRXcp* were assayed on SC medium with or without lysine. The photographs were taken after 3 days of growth at 30 °C. *C*, whole cell iron contents were measured by inductively coupled plasma spectrometry. All results shown here are the means of three independent experiments, and the *bars* indicate S.E. *D*, intracellular iron levels were measured by a QuantiChron™ iron assay kit. Shown is one representative experiment of four independent experiments. The *bars* represent S.E. ($n = 3$).

which is involved in lysine synthesis (21, 27). Previous work details that *grx5* cells fail to grow on lysine-deficient medium (21) (Fig. 4*B*). Expression of AtGRXcp rescued the lysine auxotrophy of *grx5* cells, although AtGRXcp suppression was less efficient in comparison with *Grx5*-expressing *grx5* cells (Fig. 4*B*). These results again indicate that AtGRXcp can partially restore Grx5 function in yeast cells.

AtGRXcp Suppresses Iron Accumulation in grx5 Cells—Previous studies in both yeast and zebrafish indicate that deletion of *Grx5* disrupts iron-sulfur cluster maturation and, as a consequence, iron homeostasis, which results in increased levels of intracellular iron (21, 27). This iron accumulation results in the sensitivity of *grx5* cells to external oxidants, such as H_2O_2, because of iron-mediated ROS formation (19, 21). We have demonstrated that AtGRXcp protected yeast cells against oxidative damage (Figs. 3 (*A* and *B*) and 4*A*). To further delineate the potential function of AtGRXcp, we assayed the iron content in wild type and *grx5* cells expressing vector, *Grx5*, and *AtGRXcp*. As shown in Fig. 4, *C* and *D*, *AtGRXcp-* and *Grx5*-expressing cells were both able to suppress the iron accumulation (as measured at the whole cell and intracellular levels).

Structural and Functional Analysis of the Conserved CGFS Motif—Monothiol Grxs contain a conserved putative active motif CGFS (Fig. 1) (47). To determine the importance of the CGFS domain for AtGRXcp function, we made two single-amino acid mutants ($Cys^{97} \rightarrow Ala$ change was termed AtGRXcp-AGFS, and $Phe^{99} \rightarrow Ala$ change was termed AtGRXcp-CGAS). We performed the aforementioned liquid growth assays to examine if these mutations in the conserved motif would alter AtGRXcp function. Yeast cells (*grx5*) expressing *AtGRXcp-AGFS* (*AtGRXcp-AGFS-GFP*) or *AtGRXcp-CGAS* (*AtGRXcp-CGAS-GFP*) grew similarly in YPD liquid media in comparison with vector- and *AtGRXcp*-expressing *grx5* cells (Fig. 5*A*, data not shown). However, under oxidative stress, *AtGRXcp-CGAS-*

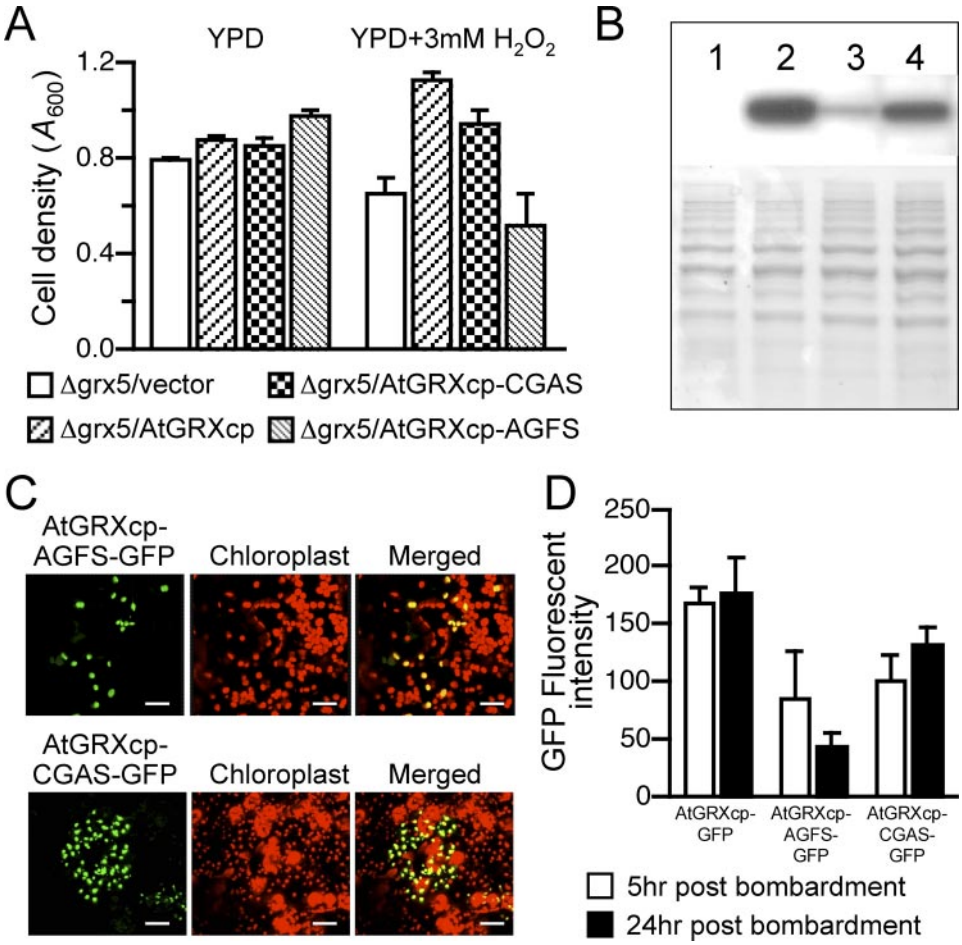

FIGURE 5. **Effect of mutations of the monothiol motif on protein expression and half-life of AtGRXcp.** *A*, vector-, *AtGRXcp-GFP-*, *AtGRXcp-AGFS-GFP-*, and *AtGRXcp-CGAS-GFP*-expressing *grx5* cells were assayed as indicated in Fig. 3. *B*, the expression of AtGRXcp and mutant variants in yeast was analyzed by Western blotting with anti-GFP antibody (1:1500). The *bottom panel* displays the protein loading stained with Coomassie Brilliant Blue. Total proteins were isolated from vector-expressing (*lane 1*), *AtGRXcp-GFP*-expressing (*lane 2*), *AtGRXcp-AGFS-GFP*-expressing (*lane 3*), and *AtGRXcp-CGAS-GFP*-expressing (*lane 4*) *grx5* cells. *C*, transient expression of AtGRXcp-AGFS-GFP and AtGRXcp-CGAS-GFP in tobacco cells at 5 h postbombardment. *Scale bars*, 20 μm (*top*) or 25 μm (*bottom*). *D*, the fluorescent intensities of AtGRXcp-GFP, AtGRXcp-AGFS-GFP, and AtGRXcp-CGAS-GFP in tobacco cells were quantified at 5 and 24 h postbombardment. *Error bars*, S.E. ($n > 100$).

(*AtGRXcp-CGAS-GFP-*) and *AtGRXcp*-expressing *grx5* cells grew significantly better than vector-expressing *grx5* cells, whereas *AtGRXcp-AGFS-* (*AtGRXcp-AGFS-GFP-*) expressing *grx5* cells grew at a slower rate than vector-expressing cells (Fig. 5*A*, data not shown). To determine if these amino acid changes ($Cys^{97} \rightarrow Ala$ and $Phe^{99} \rightarrow Ala$) affect protein expression and stability, we performed Western blots to detect AtGRXcp-GFP and the variants among yeast total proteins. Indeed, AtGRXcp-AGFS-GFP was rarely detectable, whereas AtGRXcp-CGAS-GFP levels were similar to wild type AtGRXcp (Fig. 5*B*). Those observations suggest that the $Cys^{97} \rightarrow Ala$ change may affect protein expression, which results in the inability of AtGRXcp-AGFS to suppress the sensitivity of *grx5* cells to H_2O_2. We can infer from these yeast assays that the Phe^{99} in the CGFS motif is not essential for AtGRXcp function.

We hypothesize that changes in the stability of AtGRXcp-AGFS will be similar in yeast and plant cells. To test this, we transiently expressed both mutants and AtGRXcp-GFP in tobacco cells. At 5 h postbombardment, the fluorescent intensities of the proteins were similar (Fig. 5, *C* and *D*). At 24 h postbombardment, the AtGRXcp-AGFS-GFP signal dramatically decreased, whereas there was no significant difference in signal intensity over time for the AtGRXcp-CGAS-GFP- and AtGRXcp-GFP-expressing cells (Fig. 5*D*). These findings suggest that the Cys^{97} variant alters the protein expression and the half-life of AtGRXcp similarly in both yeast and plant cells.

AtGRXcp Is Expressed in Cotyledon, Leaves, Vascular Tissues, and Flowers—Previously, RNA blot analysis indicated that *AtGRXcp* is ubiquitously expressed in *Arabidopsis* plants with high levels of *AtGRXcp* mRNA accumulating in green leaves (26). To further determine spatial and temporal *AtGRXcp* expression, the 397-bp *AtGRXcp* promoter was cloned and transcriptionally fused with the β-glucuronidase gene (GUS) and then transformed into *Arabidopsis* plants. More than 50 independent transgenic lines were generated. Preliminary GUS staining indicated that all transgenic lines harboring *AtGRXcp*::GUS had similar expression patterns (data not shown). *AtGRXcp*::GUS was highly expressed in the young cotyledons at 3 days after germination (Fig. 6*A*). In addition, *AtGRXcp*::GUS was detected in the green tissues (leaves), vascular bundles, roots, stems, and flowers (Fig. 6, *B–E*).

AtGRXcp Is Critical for Early Seedling Growth—To gain insight into the biological function of *AtGRXcp in planta*, we analyzed two Salk T-DNA insertional lines (Salk_125903 and Salk_056587) (32) carrying a T-DNA in *AtGRXcp* (Fig. 7*A*). To confirm the presence of the T-DNA in *atgrxcp* plants, we used *AtGRXcp*-specific and T-DNA-specific primers to PCR-screen T_3 progeny and obtained two homozygous lines, termed *atgrxcp1* and *atgrxcp2* (Fig. 7*A*). Sequence analysis of the T-DNA flanking regions revealed that in *atgrxcp1* the T-DNA is located in the middle of *AtGRXcp* at position Met^{71}, and in *atgrxcp 2* the T-DNA is inserted at position Ile^{12} (Fig. 7*A*). Both T-DNA insertions disrupted *AtGRXcp* expression as determined by RNA gel blot analysis (Fig. 7*B*).

Both *atgrxcp1* and *atgrxcp2* failed to display visible defects in seed germination and early growth in normal nutrient medium in comparison with wild type (Fig. 8). Given that AtGRXcp is able to restore yeast *Grx5* function (Figs. 3–5), whose mutation causes iron accumulation (21), we were interested in determining if an *AtGRXcp* deletion would affect the iron sensitivity of seedlings. Both wild type and

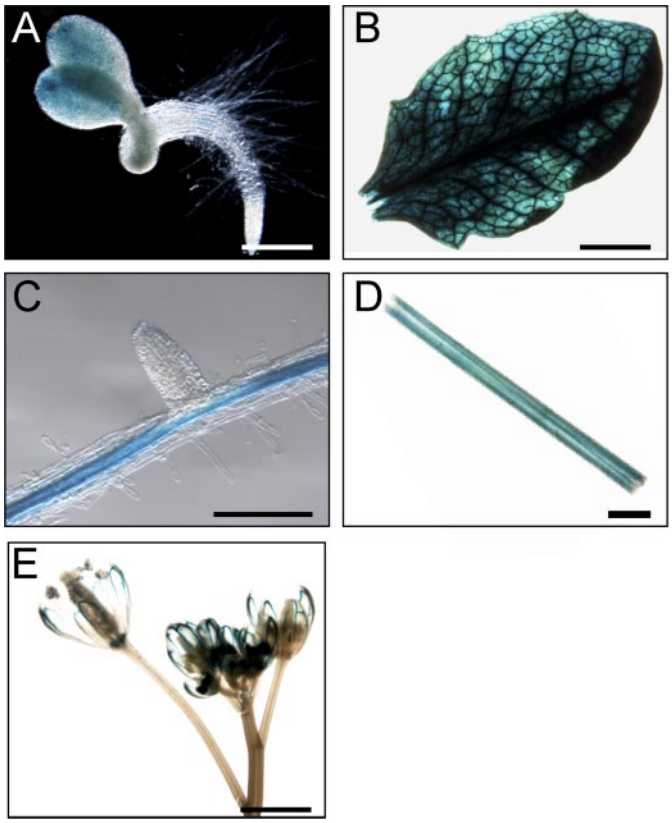

FIGURE 6. **Histochemical analyses of *Arabidopsis* plants expressing an *AtGRXcp* promoter::GUS fusion.** *A*, GUS staining in cotyledons in 3-day-old developing seedlings. *Scale bar*, 50 μm. *B*, GUS staining in rosette leaf. *Scale bar*, 2 mm. *C*, GUS staining in primary and lateral roots. *Scale bar*, 200 μm. *D*, GUS staining in vascular bundle in stems. *Scale bar*, 1 mm. *E*, GUS staining in flowers. *Scale bar*, 2 mm.

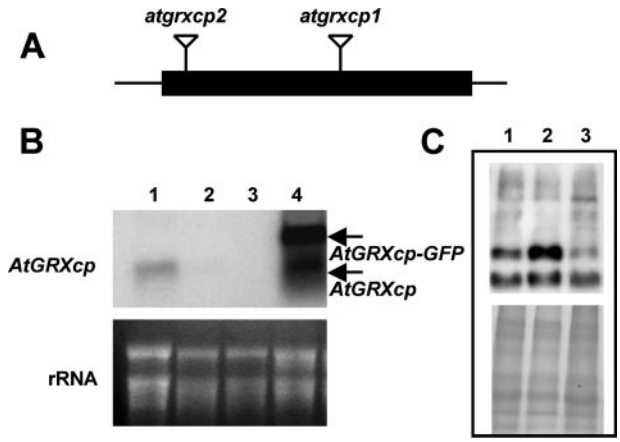

FIGURE 7. **AtGRXcp deficiency in *Arabidopsis* plants results in protein oxidative damage.** *A*, genomic structure of *AtGRXcp* showing the sites of T-DNA insertions. *B*, RNA gel blotting analysis of total RNA isolated from wild type (Col-0, *lane 1*), *atgrxcp1* (*lane 2*), *atgrxcp2* (*lane 3*), and 35S CaMV promoter-*AtGRXcp-GFP* (*lane 4*) plants, demonstrating the absences of *AtGRXcp* mRNA in both *atgrxcp* plants. The 35S CaMV promoter-AtGRXcp-GFP transgenic plants contain both endogenous *AtGRXcp* and transgene *AtGRXcp-GFP* mRNAs. *C*, protein oxidation in chloroplasts was analyzed by Western blotting as indicated in Fig. 4. *Lane 1*, wild type; *lane 2*, *atgrxcp2*; *lane 3*, 35S CaMV promoter-*AtGRXcp-GFP*.

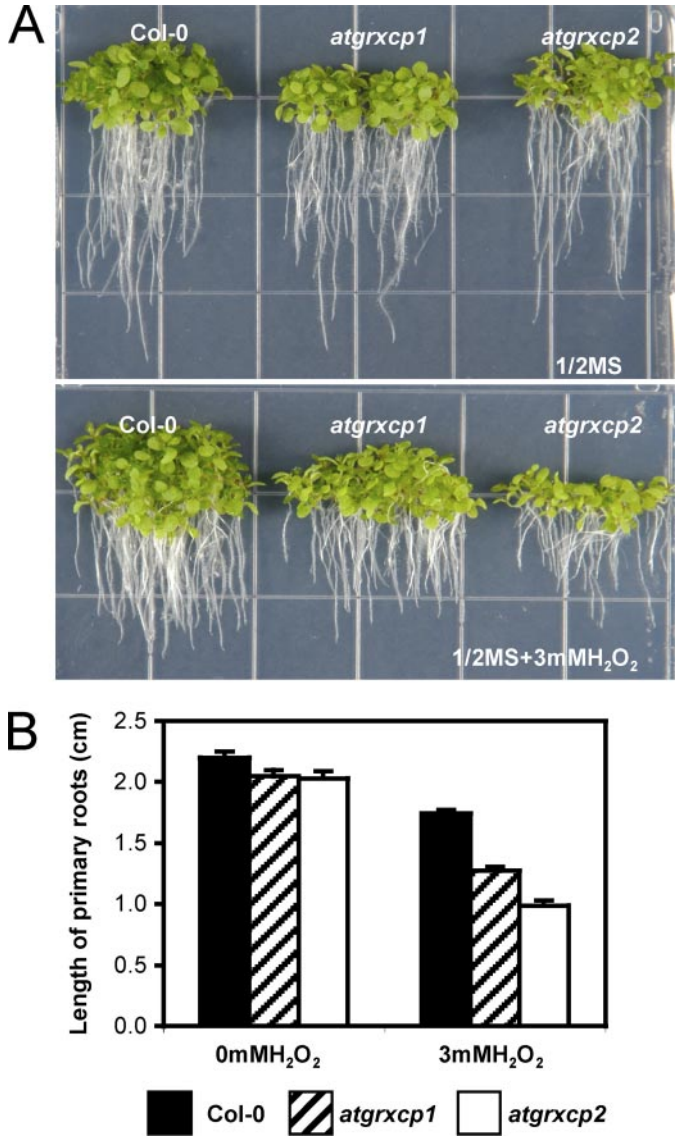

FIGURE 8. **AtGRXcp knock-out mutants are sensitive to external oxidants.** Wild type (Col-0) and *atgrxcp* allele seeds were germinated and grown on one-half strength Murashige and Skoog and the same medium supplemented with 3 mM H_2O_2 for 10 days. *A*, shown is one representative experiment of three independent experiments. *B*, root growth measurement. The length of primary roots of seedlings was measured after 10 days of growth on the medium with or without H_2O_2. *Error bars*, S.E. ($n > 50$).

atgrxcp seeds were germinated and tested on both iron-sufficient and iron-deficient media. No significant difference was seen between wild type and *atgrxcp* mutants. However, when wild type and *atgrxcp* seeds were germinated and grown on one-half strength Murashige and Skoog medium containing 3 mM H_2O_2, young seedlings of *atgrxcp* grew at a reduced rate as measured by alterations in primary root growth (Fig. 8).

Given that AtGRXcp is localized to chloroplasts, which are major sites of ROS production, we hypothesize that AtGRXcp functions in protecting against protein oxidation in chloroplasts. To test this, we isolated total chloroplast proteins from wild type-, *atgrxcp*-, and *AtGRXcp-GFP*-overexpressing plants and detected carbonyl content of the protein samples. As shown in Fig. 7*C*, the protein carbonylation for extracts from *atgrxcp* alleles was higher than that observed for extracts from wild type and *AtGRXcp-GFP*-overexpressing plants (Fig. 7*C*, data not shown).

DISCUSSION

ROS-mediated protein oxidation in chloroplasts impairs both photosynthesis and metabolic enzyme activities (1, 10). Plants have evolved a sophisticated network to scavenge ROS (2–4). Evidence presented here indicates that plant *Grx* coding sequences are similar to those found in other species, and, as we detail in this study, functional analysis also justifies the reclassification of CXIP1 to AtGRXcp (Fig. 1) (26). Our findings reveal that the first characterized plant Grx, AtGRXcp, is a functional monothiol Grx localized to chloroplasts (Fig. 2). We also demonstrate that loss of *AtGRXcp* in *Arabidopsis* leads to protein oxidation in chloroplasts and seedlings sensitive to external oxidants, such as H_2O_2 (Figs. 7 and 8), implicating a critical role of AtGRXcp in regulating redox state in chloroplasts.

A large number of Grxs have been identified in various species based solely on genome analysis (Fig. 1). In plants, several members of this protein family are predicted to target to and function in plastids/chloroplasts (30); however, little is known about their physiological roles. Both plant *AtGRXcp* and zebrafish *Grx5* are able to suppress yeast *grx5* mutant phenotypes (Figs. 3–5) (27), suggesting that the biological function of this group of monothiol glutaredoxins is evolutionarily conserved. Interestingly, AtGRXcp-GFP, like Grx5, localized to the mitochondria when expressed in yeast cells (Fig. 3*C*); however, AtGRXcp localized to chloroplasts in plant cells (Fig. 2). The dual targets of AtGRXcp have been observed for other plant and yeast proteins (45, 48). For example, the plant phosphate transporter, Pht2,1, localizes to the chloroplast envelope in plants but to mitochondria when expressed in yeast (48). The nuclear localized yeast Grx3 has been shown to be able to compensate for Grx5 when localized to the mitochondria (45). Mitochondrial localization of AtGRXcp in yeast is necessary for its function, as evidenced by the fact that when the 63-amino acid signal peptide of AtGRXcp was removed, the truncated form of AtGRXcp was unable to target mitochondria and suppress the sensitivity of *grx*5 cells to H_2O_2 (Fig. 3).

The ability of AtGRXcp to partially restore the Fe-S enzyme activities and suppress iron accumulation in yeast *grx5* cells suggests that AtGRXcp may be required for biogenesis of iron-sulfur (Fe-S) clusters and/or involved in the regulation of iron homeostasis in chloroplasts. In plants, Fe-S clusters have an important role in the light-harvesting photosystem I and the cytochrome b_6/f complex for electron transport (49). Chloroplasts/plastids also contain many Fe-S proteins, such as a 2Fe-2S ferredoxin and 4Fe-4S ferredoxin-thioredoxin reductase (50). Recent studies indicate that *Arabidopsis* proteins directly and indirectly linked to chloroplast activities exhibit more sensitivity to oxidative damage (9). There is a possibility that AtGRXcp protects protein oxidative damage via modulating iron homeostasis to control iron-generated oxygen radicals within chloroplasts. Support for this model was observed in *AtGRXcp*-expressing yeast cells. Apparently, AtGRXcp attenuates protein oxidation by reducing intracellular iron levels (Fig. 4, C and *D*). Furthermore, in plants, proteins from chloroplasts of *atgrxcp* plants were subjected to increased carbonylation, an indicator of increased oxidative damage to proteins (Fig. 7*C*). It is also possible that AtGRXcp suppression of yeast *grx5* mutant phenotypes was due to activation of the ROS scavenging system (Figs. 3 and 4). In support of this hypothesis, recent studies indicate that monothiol Grxs can modulate cellular signaling events through protein-protein interactions mediated by PICOT-HD (23, 26, 51). Future work will be necessary to determine the target(s) of AtGRXcp and understand the complexity of ROS regulation *in planta*.

AtGRXcp contains the putative active motif, CGFS (Fig. 1), and substitution of the conserved cysteine residue (Cys^{97}) with alanine caused a deceased expression and shorter half-life of AtGRXcp in both yeast and plant cells (Fig. 5, *B–D*). In contrast, mutation of both the conserved Cys^{60} and the nonconserved Cys^{117} in yeast Grx5 and the conserved Cys^{30} in bacterial Grx4 did not significantly affect protein stability (20, 47, 52). These findings suggest that this particular cysteine residue (Cys^{97}) may play a unique role in the plant AtGRXcp. In addition, our results suggest that the conserved phenylalanine residue (Phe^{99}) is not essential for the function of AtGRXcp (Fig. 6). In this case, our findings are similar to that observed with the Phe^{62} variants in yeast Grx5 (47). Recently, the resolved three-dimensional solution structure of the bacterial Grx4 reveals that this monothiol Grx has a unique structure, which is significantly different from the dithiol Grxs (53). AtGRXcp consists of four cysteine residues: the conserved Cys^{97} and the nonconserved Cys^{151}, which are located in the conserved GRX region (Fig. 1), and two additional cysteine residues (Cys^{62} and Cys^{172}) that are not conserved in the monothiol Grxs (Fig. 1) (26). Future work will need to be directed at the various roles these cysteine residues may have in disulfide formation, electron donation, and redox-catalysis.

We have already pursued several avenues to further discern the biochemical properties of AtGRXcp. Initial analysis indicated that AtGRXcp, like yeast Grx5 and bacterial Grx4, was not active in either the insulin or the β-hydroxyethyl disulfide assays (data not shown) (20, 52). We certainly envision AtGRXcp playing a myriad of roles *in planta*; however, studies directed at clarifying other AtGRXcp functions require additional inquiry.

Recent reports have shown that *Arabidopsis* has high steady-state levels of protein carbonylation, particularly chloroplastic proteins, during vegetative growth (9, 54). *AtGRXcp* is highly expressed in young cotyledons, green leaves, and the vasculature of roots (Fig. 6, *A–C*), implicating that *AtGRXcp* may be critical for protecting chloroplasts/plastids against oxidative damage during early growth and development. In agreement with this, *atgrxcp* mutant roots are more sensitive to external oxidants (Fig. 8). It is possible that plastidic AtGRXcp could be involved in the glutathiolation/deglutathiolation of proteins through coupling with GSH and GSH reductase in chloroplasts/plastids, which is required for early seedling growth (55). This hypothesis is reinforced by results suggesting that changes in glutathione redox state controlled via GSH reductase activities have an important role in cell differentiation, root growth, and plant development (56, 57). In addition, a CC type Grx, ROXY1, appears to play a role in post-translational regulation of floral identity gene products that are required for floral petal development (31).

Although *atgrxcp* plants did not display any altered sensitivity to iron imbalance at the whole plant level (data not shown), this may be due to tight regulation of iron uptake (34) or iron-related phenotypes being masked by functional redundancy among Grxs (12, 30). The interplay among Grxs and various antioxidant systems will also be addressed in future studies.

The characterization of *AtGRXcp* reported here is particularly noteworthy in that Grxs have not been previously functionally characterized. AtGRXcp appears to be evolutionarily conserved across taxa, and the capability of AtGRXcp to rescue yeast *Grx5* deficiency phenotypes suggests a conserved biochemical mechanism among monothiol Grxs. The *AtGRXcp*-deficient plant lines demonstrate that this protein plays a critical role in protecting protein oxidation during stress conditions. Given that there are at least 31 genes in the *Arabidopsis* genome coding glutaredoxins, the characterization of AtGRXcp is an important first step toward understanding how this large gene family functions in adapting plants to external stresses.

Acknowledgments—We thank Dr. Enrique Herrero for wild type and grx yeast strains, Dr. Elison Blancaflor for providing the Golgi marker construct, Dr. Toshiro Shigaki for phylogenetic analysis, Adam Gillum for graphics, and Dr. Jon Pittman, Dr. Jian Zhao, and Jay Morris for critical reading of the manuscript.

REFERENCES

1. Apel, K., and Hirt, H. (2004) *Annu. Rev. Plant Biol.* **55,** 373–399
2. Vranová, E., Inzé, D., and Van Breusegem, F. (2002) *J. Exp. Bot.* **53,** 1227–1236
3. Rhoads, D. M., Umbach, A. L., Chalivendra, S. C., and Siedow, J. N. (2006) *Plant Physiol.* **141,** 357–366
4. Foyer, C. H., and Noctor, G. (2005) *Plant Cell* **17,** 1866–1875
5. Fobert, P. R., and Després, C. (2005) *Curr. Opin. Plant Biol.* **8,** 378–382
6. Gechev, T. S., and Hille, J. (2005) *J. Cell Biol.* **168,** 17–20
7. Finkel, T., and Holbrook, N. J. (2000) *Nature* **408,** 239–247
8. Nyström, T. (2005) *EMBO J.* **24,** 1311–1317
9. Johansson, E., Olsson, O., and Nyström, T. (2004) *J. Biol. Chem.* **279,** 22204–22208
10. Buchanan, B. B., and Balmer, Y. (2005) *Annu. Rev. Plant Biol.* **56,** 187–220
11. Fernandes, A. P., and Holmgren, A. (2004) *Antioxid. Redox Signal.* **6,** 63–74
12. Rouhier, N., Gelhaye, E., and Jacquot, J.-P. (2004) *Cell Mol. Life. Sci.* **61,** 1266–1277
13. Holmgren, A., and Åslund, F. (1995) *Methods Enzymol.* **252,** 283–292
14. Holmgren, A. (1989) *J. Biol. Chem.* **264,** 13963–13966
15. Bushweller, J. H., Åslund, F., Wüthrich, K., and Holmgren, A. (1992) *Biochemistry* **31,** 9288–9293
16. Ortenberg, R., Gon, S., Porat, A., and Beckwith, J. (2004) *Proc. Natl. Acad. Sci. U. S. A.* **101,** 7439–7444
17. Grant, C. M. (2001) *Mol. Microbiol.* **39,** 533–541
18. Lillig, C. H., Berndt, C., Vergnolle, O., Lönn, M. E., Hudemann, C., Bill, E., and Holmgren, A. (2005) *Proc. Natl. Acad. Sci. U. S. A.* **102,** 8168–8173
19. Rodrígues-Manzaneque, M. T., Ros, J., Cabiscol, E., Sorribas, A., and Herrero, E. (1999) *Mol. Cell. Biol.* **19,** 8180–8190
20. Fernandes, A. P., Fladvad, M., Berndt, C., Andrésen, C., Lillig, C. H., Neubauer, P., Sunnerhagen, M., Holmgren, A., and Vlamis-Gardikas, A. (2005) *J. Biol. Chem.* **280,** 24544–24552
21. Rodríguez-Manzaneque, M. T., Tamarit, J., Bellí, G., Ros, J., and Herrero, E. (2002) *Mol. Biol. Cell* **13,** 1109–1121
22. Jablonowski, D., Butler, A. R., Fichtner, L., Gardiner, D., Schaffrath, R., and Stark, M. J. R. (2001) *Genetics* **159,** 1479–1489
23. Lopreiato, R., Facchin, S., Sartori, G., Arrigoni, G., Casonato, S., Ruzzene, M., Pinna, L. A., and Carignani, G. (2004) *Biochem. J.* **377,** 395–405
24. Witte, S., Villalba, M., Bi, K., Liu, Y., Isakov, N., and Altman, A. (2000) *J. Biol. Chem.* **275,** 1902–1909
25. Rahlfs, S., Fischer, M., and Becker, K. (2001) *J. Biol. Chem.* **276,** 37133–37140
26. Cheng, N.-H., and Hirschi, K. D. (2003) *J. Biol. Chem.* **278,** 6503–6509
27. Wingert, R. A., Galloway, J. L., Barut, B., Foott, H., Fraenkel, P., Axe, J. L., Weber, G. J., Dooley, K., Davidson, A. J., Schmid, B., *et al.* (2005) *Nature* **436,** 1035–1039
28. Isakov, N., Witte, S., and Altman, A. (2000) *Trends Biochem. Sci.* **25,** 537–539
29. Rouhier, N., Vlamis-Gardikas, A., Lillig, C. H., Berndt, C., Schwenn, J.-D., Holmgren, A., and Jacquot, J.-P. (2003) *Antioxid. Redox Signal.* **5,** 15–22
30. Lemaire, S. D. (2004) *Photosynth. Res.* **79,** 305–318
31. Xing, S., Rosso, M. G., and Zachgo, S. (2005) *Development* **132,** 1555–1565
32. Alonso, J. M., Stepanova, A. N., Leisse, T. J., Kim, C. J., Chen, H., Shinn, P., Stevenson, D. K., Zimmerman, J., Barajas, P., Cheuk, R., *et al.* (2003) *Science* **301,** 653–657
33. Murashige, T., and Skoog, F. (1962) *Physiol. Plant* **15,** 473–497
34. Vert, G., Grotz, N., Dédaldéchamp, F., Gaymard, F., Guerinot, M. L., Briat, J.-F., and Curie, C. (2002) *Plant Cell* **14,** 1223–1233
35. Shigaki, T., Cheng, N.-H., Pittman, J. K., and Hirschi, K. (2001) *J. Biol. Chem.* **276,** 43152–43159
36. Nathan, D. F., Vos, M. H., and Lindquist, S. (1999) *Proc. Natl. Acad. Sci. U. S. A.* **96,** 1409–1414
37. Ausubel, F., Brent, R., Kingston, R. E., Moore, D. D., Seidman, J. G., Smith, J. A., ane Struhl, K. (1996) *Current Protocols in Molecular Biology*, Vol. 2, pp. 13.7.1–13.7.5, John Wiley & Sons Inc., Hoboken, NJ
38. Cheng, N.-H., Liu, J.-Z., Nelson, R. S., and Hirschi, K. D. (2004) *FEBS Lett.* **559,** 99–106
39. Trelease, R. N., Lee, M. S., Banjoko, A., and Bunkelmann, J. (1995) *Protoplasma* **195,** 156–167
40. Cheng, N.-H., Pittman, J. K., Barkla, B. J., Shigaki, T., and Hirschi, K. D. (2003) *Plant Cell* **15,** 347–364
41. Levine, R. L., Williams, J. A., Stadtman, E. R., and Shacter, E. (1994) *Methods Enzymol.* **233,** 346–357
42. Davletova, S., Rizhsky, L., Liang, H., Zhong, S., Oliver, D. J., Coutu, J., Shulaey, V., Schlauch, K., and Mittler, R. (2005) *Plant Cell* **17,** 268–281
43. Fitzpatrick, L. M., and Keegstra, K. (2001) *Plant J.* **27,** 59–65
44. Havlin, J. L., and Soltanpour, P. N. (1989) *Commun. Soil Sci. Plant Anal.* **14,** 969–980
45. Molina, M. M., Bellí, G., de la Torre, M. A., Rodríguez-Manzaneque, M. T., and Herrero, E. (2004) *J. Biol. Chem.* **279,** 51923–51930
46. Mühlenhoff, U., Gerber, J., Richhardt, N., and Lill, R. (2003) *EMBO J.* **22,** 4815–4825
47. Bellí, G., Polaina, J., Tamarit, J., de la Torre, M. A., Rodríguez-Manzaneque, M. T., Ros, J., and Herrero, E. (2002) *J. Biol. Chem.* **277,** 37590–37596
48. Versaw, W. K., and Harrison, M. J. (2002) *Plant Cell* **14,** 1751–1766
49. Balk, J., and Lobréaux, S. (2005) *Trends Plant Sci.* **10,** 324–331
50. Buchanan, B. B., Schurmann, P., Wolosiuk, R. A., and Jacquot, J.-P. (2002) *Photosynth. Res.* **73,** 215–222
51. Bécamel, C., Alonso, G., Galéotti, N., Demey, E., Jouin, P., Ullmer, C., Dumuis, A., Bockaert, J., and Marin, P. (2002) *EMBO J.* **21,** 2332–2342
52. Tamarit, J., Bellí, G., Cabiscol, E., Herrero, E., and Ros, J. (2003) *J. Biol. Chem.* **278,** 25745–25751
53. Fladvad, M., Bellanda, M., Fernandes, A. P., Mammi, S., Vlamis-Gardikas, A., Holmgren, A., and Sunnerhagen, M. (2005) *J. Biol. Chem.* **280,** 24553–24561
54. Job, C., Rajjou, L., Lovigny, Y., Belghazi, M., and Job, D. (2005) *Plant Physiol.* **138,** 790–802
55. Ogawa, K. (2005) *Antioxid. Redox Signal.* **7,** 973–981
56. Henmi, K., Demura, T., Tsuboi, S., Fukuda, H., Iwabuchi, M., and Ogawa, K. (2005) *Plant Cell Physiol.* **46,** 1757–1765
57. Yanagida, M., Mino, M., Iwabuchi, M., and Ogawa, K. (2004) *Plant Cell Physiol.* **45,** 129–137